Mon. Not. R. Astron. Soc. **266**, 114–122 (1994)

A near-infrared photometric study of the young Orion nebula star cluster NGC 1976

Z. Y. Qian[1]* and R. Sagar[2]†
[1] *Beijing Astronomical Observatory, Chinese Academy of Sciences, Beijing 100080, China*
[2] *Indian Institute of Astrophysics, Bangalore 560034, India*

Accepted 1993 July 8. Received 1993 July 1; in original form 1993 March 9

ABSTRACT

We have measured the *JHK* magnitudes of 47 stars in the region of the extremely young Orion nebula star cluster NGC 1976. These, in combination with the existing near-infrared and optical data, are used to study the intracluster extinction law. This indicates an anomalous distribution of intracluster grains in the vicinity of many stars causing less extinction in the *U*, *B*, *R* and *I* passbands than that obtained from the colour excess $E(V-J)$ using a normal interstellar extinction law. This implies a small shift in the grain size distribution towards larger than normal sized particles in these regions.

Key words: dust, extinction – ISM: general – open clusters and associations: individual: NGC 1976 – infrared: general.

1 INTRODUCTION

The extremely young Orion nebula star cluster (≡the Trapezium star cluster≡M42≡NGC 1976≡C 0532−054) is embedded within the Orion nebula and includes the Trapezium stars. The cluster contains massive stars with spectral types as early as O7 as well as very-low-mass stars visible only on long exposures at infrared wavelengths. The cluster itself is embedded in a massive complex of gas including neutral, ionized and molecular material and several objects such as spectroscopic binaries, masers and infrared objects. Since the Orion complex is very young ($\sim 10^6$ yr) and near to the Sun, it is the obvious reference point for investigations of the formation of stars and clusters. Located near the Celestial Equator, Orion is a good candidate for observations from both the northern and southern hemispheres and therefore has an excellent observational history.

The cluster has been extensively studied photometrically (see Sharpless 1952, 1954, 1962; Lee 1968; Walker 1969, 1983; Warren & Hesser 1977a, b) as well as spectroscopically (see Smith 1972; McNamara 1976; Levato & Abt 1976; Abt, Wang & Cardona 1991; and references therein). For a complete list of references, one can refer to the latest catalogue by Mermilliod (1992). These optical as well as near-infrared (IR) photometric and polarimetric studies of the cluster (see Lee 1968; Walker 1983; Breger, Gehrz & Hackwell 1981; and references therein) indicate the presence of non-uniform extinction across the cluster region, which is not surprising in view of the extremely young age of ~1 Myr of the cluster (Herbig & Terndrup 1986). The values of the $E(B-V)$ colour excess for the cluster members show a large variation, ranging from ~0.02 to 1.0 mag (cf. Sagar 1987 and references therein). Panek (1983) studied the ultraviolet flux distribution of 15 early-type stars of the cluster, but derived extinction curves for only six stars with $E(B-V)>0.2$ mag.

In most of the earlier studies of extinction in which near-IR observations were used, cluster members could not be reliably separated from field stars due to lack of accurate proper motion (PM) data. Recently, such data have been provided by Van Altena et al. (1988) and Jones & Walker (1988) in the central (the Trapezium) region and by McNamara et al. (1989) in the outer region of the cluster.

This paper studies the extinction due to intracluster material using multiwavelength observations of PM cluster members. We have carried out *JHK* photometry of 47 stars in the cluster region, most of which are heavily reddened stars. Near-IR photometry has proved to be a useful tool for such studies (see Tapia et al. 1984, 1988, 1991; Smith 1987; Roth 1988; Sagar & Qian 1989, 1990), especially when combined with observations at other wavelengths.

The stars in the cluster area have been numbered by Brun (1935) and Parenago (1954); we shall use the latter's numbering.

*Deceased 1993 June 16.
†E-mail address: sagar@iiap.ernet.in.

2 OBSERVATIONS AND REDUCTIONS

47 stars brighter than $V=14$ mag and generally having a high (≥ 50 per cent) probability of cluster PM membership are selected for the present observations. Most of them have $E(B-V) \geq 0.20$ mag, which is large in comparison to the cluster foreground reddening of $E(B-V)=0.05$ mag (cf. Breger et al. 1981).

The *JHK* photometric observations were carried out by one of us (ZYQ) between 1990 December and 1991 February on the $f/30$ Cassegrain focus of the 1.26-m infrared telescope of Beijing Astronomical Observatory located at the Xinglong Station. An InSb detector was employed. The details of the instruments used for the observations are given elsewhere (Hu 1986; Sagar & Qian 1989). Stars were generally observed with an aperture size of 16 arcsec diameter and with a chopping amplitude of 60 arcsec. The effective wavelengths, and the bandwidths at half maximum (given inside the bracket), of the filters *J*, *H* and *K* in μm are 1.26 (0.25), 1.68 (0.40) and 2.28 (0.48) respectively.

Instrumental magnitudes were first corrected for atmospheric extinction and then converted to the standard system in the same way as described by Sagar & Qian (1989).

The error in the *JHK* magnitudes for a single observation was estimated as $[(1.09/SN)^2+E^2]^{1/2}$, where SN is the signal-to-noise ratio and E is the error in fixing the zero-point of the photometric system. The infrared standard star HD 40335 was used to estimate the nightly zero-point for the programme stars. The accuracy of the zero-point is better than 0.04 mag in all three passbands. This is the main source of error in the *JHK* magnitudes of stars brighter than 9.0 mag, while poor signal-to-noise ratio is the major source of error in the observations of faint stars. The stars have generally been observed twice on different nights. The weighted average of the observations along with the errors is given in Table 1.

We compared our observations with those of Breger et al. (1981), and found no systematic variation of the differences with either *J* magnitude or $(J-H)$ colour. The statistical results of the comparison are given in Table 2. A few stars, discussed below, discrepant by more than 3σ have been excluded from the analysis. The largest discrepancies are -0.48 in *J* magnitude for star 1956; -0.47 and -0.37 in *H* magnitude for stars 1712 and 1956 respectively; and 1.20, -0.51 and -0.49 in *K* magnitude for stars 2368, 1683 and 1956 respectively. These are either emission-line stars or variables or both (Mermilliod 1992; McNamara & Huels 1983). The biggest change has been observed in the *K* magnitude of a known flare star 2368. Considering the errors in the observations as well as the fact that the cluster is embedded in a nebular region, we conclude that the agreement between the two sets of data is satisfactory, except for the stars discussed above.

Proper motion studies are supposed to separate cluster members from field stars more effectively than other commonly used methods, namely photometric and/or statistical methods, if the accuracy of the determination is high enough to separate the cluster motion from the motion of field stars. A number of PM studies have therefore been carried out recently for the Orion nebula region. Most of these have been concentrated on a relatively small area centred on the Trapezium (McNamara 1976; Jones & Walker 1988; Van

Table 1. *JHK* magnitudes of the programme stars. Star numbers are according to Parenago (1954). The cluster membership probability (p) is taken from McNamara et al. (1989), if available. Otherwise it is taken from McNamara & Huels (1983) and is asterisked.

Star	J±σ (mag)	H±σ (mag)	K±σ (mag)	p (%)	V (mag)	Spectral Type
1044	7.54±0.02	7.56±0.02	7.67±0.03	80	7.67	B2.5 IV
1049	8.77±0.04	8.04±0.02	7.91±0.03	85	11.87	K2 IV
1212	9.71±0.06	9.28±0.05	9.52±0.07	30	11.39	A0 V
1281	9.54±0.06	9.42±0.06	9.49±0.08	93	10.72	F3 IV
1360	11.17±0.19	11.66±0.27	–	87*	13.81	G8 V
1391	9.69±0.06	9.51±0.06	9.36±0.07	83	10.31	F7 IV
1409	9.39±0.05	8.90±0.04	8.45±0.04	85	11.57	F8 V ne
1469	9.77±0.06	9.08±0.05	8.82±0.04	0	12.26	G9 IV-V
1511	9.22±0.04	9.00±0.04	8.99±0.05	93	9.30	A2 V
1513	9.81±0.05	10.06±0.05	9.98±0.04	0	10.56	A3 V
1539	9.10±0.04	8.87±0.04	8.88±0.04	88	10.77	A0 V
1683	10.11±0.10	9.89±0.08	9.48±0.09	57	10.93	A0 V
1699	10.50±0.20	9.98±0.12	9.43±0.13	0	13.04	G0 V
1708	7.39±0.02	7.40±0.03	7.44±0.03	77	7.35	B3 V
1712	9.16±0.05	8.85±0.05	8.73±0.05	77	10.47	A0 V
1736	8.18±0.02	7.57±0.03	7.31±0.02	89	11.11	G5 III
1772	7.70±0.01	7.50±0.03	7.32±0.03	96*	8.46	B2 V
1798	8.37±0.05	8.06±0.05	7.80±0.04	91	9.47	B3 V n
1799	9.68±0.07	8.82±0.05	8.69±0.04	18	12.52	F0 IV
1854	9.02±0.04	8.84±0.05	8.81±0.05	95*	10.10	A0 V
1863	5.63±0.02	5.33±0.01	5.35±0.02	95*	8.03	B3 V
1865	4.80±0.02	4.61±0.01	4.73±0.04	96*	6.74	O7 V
1881	8.76±0.03	8.79±0.04	8.76±0.06	82	9.81	A0 V
1885	9.30±0.06	8.95±0.05	8.81±0.05	93*	10.55	A2 V
1889	5.95±0.03	5.83±0.01	5.62±0.03	96*	6.68	B0.5 V
1891	4.51±0.01	4.33±0.01	4.18±0.00	96*	5.14	O6 V
1955	8.80±0.05	8.18±0.03	8.20±0.04	93	10.91	G2 III
1956	7.86±0.02	7.34±0.01	7.05±0.01	90*	9.63	B2 V
1993	4.78±0.01	4.83±0.01	4.86±0.01	93*	5.06	O9 V
2001	10.12±0.11	9.65±0.06	9.88±0.08	83	12.38	G8 V
2029	8.73±0.05	7.68±0.02	6.92±0.02	8	12.26	G3 IV-V
2033	9.68±0.05	9.24±0.02	9.09±0.02	94*	11.73	G3 IV-V
2069	10.47±0.15	9.96±0.12	9.84±0.14	85	12.04	G8 V
2074	5.76±0.01	5.58±0.01	5.51±0.03	94*	6.83	B0.5 V
2100	9.45±0.05	8.68±0.03	8.56±0.04	84	11.77	G9 IV-V
2181	10.13±0.10	9.57±0.05	9.11±0.06	89	12.62	K2 V e
2244	10.06±0.09	9.38±0.04	9.59±0.06	83	12.35	K1 V e
2247	8.49±0.03	7.40±0.01	6.40±0.00	75	10.00	A3 V p
2248	8.93±0.05	8.43±0.03	8.10±0.03	83	11.31	B9 V
2302	9.38±0.09	9.27±0.09	9.23±0.09	86	9.94	B9 V
2317	10.57±0.13	10.73±0.17	10.32±0.14	0	12.49	F6 IV
2368	11.07±0.20	10.96±0.18	10.81±0.19	89	13.56	K4 IV-V e
2424	9.72±0.08	9.66±0.08	9.75±0.09	0	10.74	A4 V
2425	8.77±0.05	8.32±0.03	8.16±0.04	92	10.67	B6 V
2476	9.25±0.04	8.70±0.01	8.44±0.01	95*	12.83	G5 III
2500	10.44±0.10	10.34±0.05	10.44±0.07	41	11.34	A3 V
2519	9.53±0.10	9.51±0.08	9.25±0.08	52	11.27	A0 V

Table 2. Statistical results of the photometric comparison with Breger et al.'s (1986) data. The difference is always in the sense of our minus Breger et al.'s data. The mean and standard deviation (σ) are based on *N* stars.

Differences in	Mean (mag)	σ (mag)	N
J	-0.01	0.16	7
H	-0.05	0.08	8
K	-0.08	0.18	25
(J-H)	-0.06	0.06	4
(J-K)	0.07	0.16	8
(H-K)	-0.03	0.15	10

Altena et al. 1988). The most extensive PM studies of stars outside the central Orion emission region are that by Parenago (1954), and more recently that by McNamara et al. (1989). Using Parenago's PM data, McNamara & Huels (1983) assigned a cluster membership probability (p) to the stars in NGC 1976. On this scale, all the programme stars have $p \geq 50$ per cent with a median p of 96 per cent, indicating that only two stars of our sample could be field stars, while according to McNamara et al. (1989) five of our programme stars have $p = 0$ per cent and another four have $p < 50$ per cent (cf. Table 1). In the light of these we conclude that the number of field stars that might be present among the programme stars is not statistically significant.

We find from the infrared catalogue of Gezari, Schmitz & Mead (1987) that, besides our programme stars, more than 155 stars in the cluster region have both PM data and observations in at least two of the five near-IR (*JHKLM*) bands. For separating field stars from this sample, we used the p values given by van Altena et al. (1988) and McNamara et al. (1989) in the central and outer regions respectively. We considered those 118 stars that have $p \geq 50$ per cent as cluster members and included them in further analysis. For these as well as for our programme stars, the *UBVRI* photoelectric photometric and MKK spectral classification data were taken from the catalogue of open star clusters distributed by Mermilliod (1992) on magnetic tape, while the *JHKLM* data, except for the *JHK* values given in Table 1, were taken from Gezari et al. (1987).

The V, $(B-V)$ and V, $(V-K)$ colour–magnitude diagrams and the $(V-K)$, $(B-V)$ and $(J-H)$, $(H-K)$ colour–colour diagrams are plotted in Figs 1 and 2 respectively. The location of the zero-age main sequence given by Schmidt-Kaler (1982) is shown in Fig. 1. The apparent distance modulus to the cluster, $(m-M)$, has been taken as 8.15 mag (cf. Breger et al. 1981). The location of a small number of stars below the zero-age main sequence in the V, $(B-V)$, the V, $(V-K)$ and the $(V-K)$, $(B-V)$ diagrams can be accounted for in terms of either photometric errors or some peculiarities. Photometric errors are ~ 0.05 mag for the photoelectric V and $(B-V)$ data, but they are ~ 0.1 mag in the case of the J, H and K magnitudes (cf. Table 1). Many stars lie significantly above the main sequence. Clearly, in Fig. 2 there is a large scatter in the direction of the reddening vector, implying a considerable amount of differential interstellar extinction across the cluster.

In the $(J-H)$ versus $(H-K)$ diagram, the positions of a few stars are peculiar in the sense that the $(H-K)$ colours are either too blue or too red for the corresponding $(J-H)$ colours. These stars will be discussed in detail later.

3 INTERSTELLAR EXTINCTION TO THE CLUSTER

To study the extinction of the cluster members, we derive $E(U-V)$, $E(B-V)$, $E(V-R)$, $E(V-I)$, $E(V-J)$, $E(V-H)$, $E(V-K)$, $E(V-L)$ and $E(V-M)$ colour excesses. We obtain these by comparing the observed colours of a star with its intrinsic colours derived from the MKK spectral-type–luminosity-class colour relations given by FitzGerald (1970) for $(U-B)$ and $(B-V)$; by Johnson (1966) for $(V-R)$ and $(V-I)$; and by Koornneef (1983) for $(V-J)$, $(V-H)$, $(V-K)$, $(V-L)$ and $(V-M)$ colours. $E(U-V)$, $E(B-V)$, $E(V-R)$ and $E(V-I)$ are generally uncertain by ~ 0.07 mag, while $E(V-J)$, $E(V-H)$, $E(V-K)$, $E(V-L)$ and $E(V-M)$ have typical errors of ~ 0.15 mag. This is

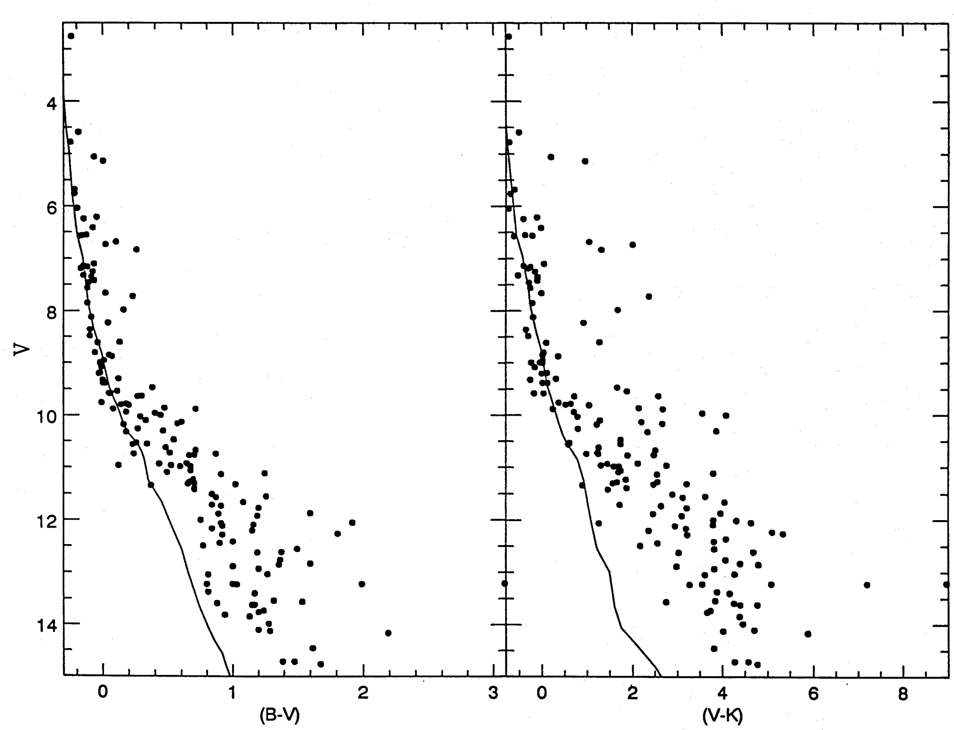

Figure 1. The V, $(B-V)$ and V, $(V-K)$ colour-magnitude diagrams for cluster members having near-infrared observations. Continuous curves give the location of the intrinsic main sequence.

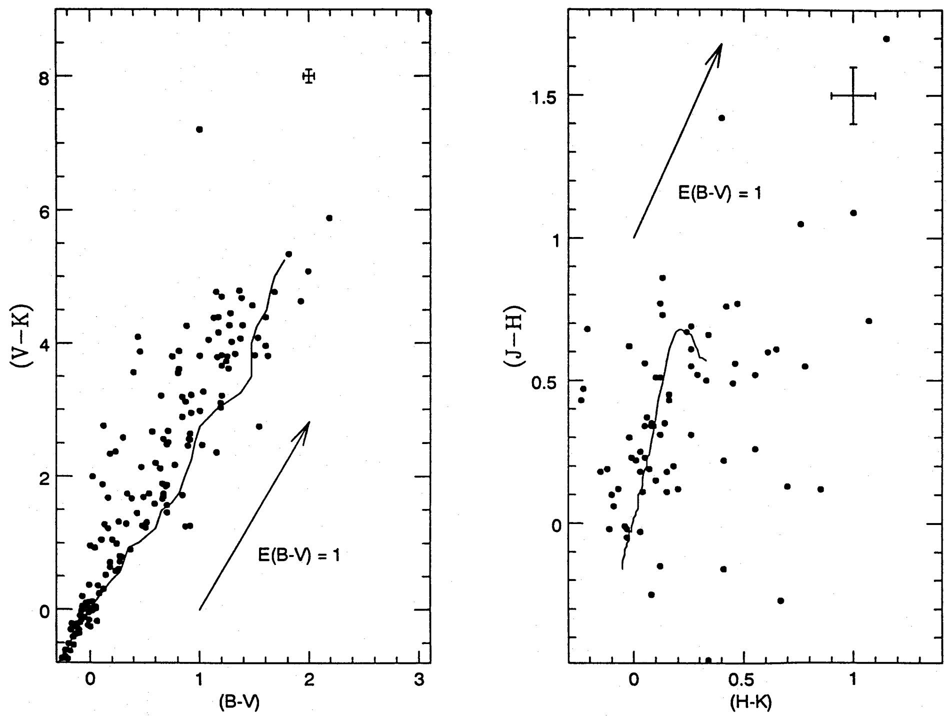

Figure 2. The $(V-K)$, $(B-V)$ and $(J-H)$, $(H-K)$ colour–colour diagrams for cluster members having near-infrared data. The lengths of the crosses represent the observational errors (σ). Continuous curves give the intrinsic main sequence. The standard reddening vectors for $E(B-V)=1$ mag are shown by arrows.

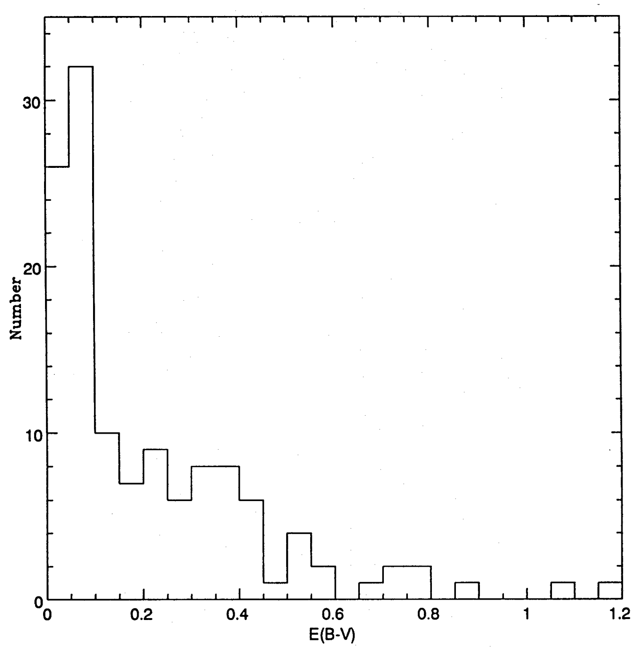

Figure 3. A histogram of the $E(B-V)$ colour excess.

mainly because *UBVRI* magnitudes are more accurate than *JHKLM* magnitudes. Fig. 3 shows the histogram of $E(B-V)$. For a few stars, the value of $E(B-V)$ is larger than 1.0 mag. However, a good fraction (~ 45 per cent) of the cluster members have $E(B-V)<0.10$ mag. This agrees very well with the earlier findings (cf. Lee 1968; Walker 1969; Penston 1973; Breger 1976; Sagar 1987) that, from the point of view of interstellar extinction, cluster members fall into two groups, namely (1) the stars located in front of the Orion clouds, which are affected by a small and approximately constant reddening, $E(B-V)$, and (2) the stars situated within or behind the Orion complex of H II regions and molecular clouds, which have much larger values of $E(B-V)$ than the foreground stars.

4 EXTINCTION DUE TO INTRACLUSTER MATERIAL

The observed colour excesses of the stars situated within or behind the Orion clouds can be considered as the sum of the foreground interstellar and intracluster extinctions. The observed $E(V-J)$ colour excesses of such stars, for example, can be written as

$$E(V-J)=FE(V-J)+IE(V-J),$$

where $FE(V-J)$ and $IE(V-J)$ are the $(V-J)$ colour excess due to foreground interstellar and intracluster materials respectively. In order to understand the properties of intracluster material, we use the $IE(U-V)$, $IE(B-V)$, $IE(V-R)$, $IE(V-I)$, $IE(V-J)$, $IE(V-H)$, $IE(V-K)$, $IE(V-L)$ and $IE(V-M)$ colour excesses of only those cluster members that have $E(B-V)>0.10$ mag, and analyse them in the following way.

4.1 Correction for foreground interstellar extinction

From optical and near-IR photometry and optical polarimetric observations, Breger et al. (1981) found that the foreground interstellar matter follows the normal extinction law, with values of $R[\approx A_v/FE(B-V)]=3$ and $FE(B-V)=0.05$ mag. These values and the optical–near-IR reddening law given by Mathis (1990) have been used here to derive the $FE(U-V)$, $FE(V-R)$, $FE(V-I)$, $FE(V-J)$, $FE(V-H)$, $FE(V-K)$, $FE(V-L)$ and $FE(V-M)$ colour excesses due to foreground interstellar matter. These values were subtracted from the corresponding observed colour excesses to derive the corresponding colour excesses due to intracluster material.

4.2 Colour excess diagrams

Recent studies of the interstellar extinction law use parameters such as $E(V-J)$ and $E(V-K)$, instead of $E(B-V)$ (Smith 1987; Tapia et al. 1988, 1991; Sagar & Qian 1989, 1990), because they do not depend on environmental properties such as the chemical composition, the shape, the structure and the degree of alignment of the interstellar matter (Voshchinnikov & Il'in 1987; Cardelli, Clayton & Mathis 1989; Mathis 1990, and references therein). These parameters are also better measures of the total amount of interstellar extinction, due to their large values compared to either near-IR or optical colour excesses. The colour excess used as a measure of interstellar extinction should, however, be selected carefully as the cluster is embedded in emission nebulosity and also contains young stellar objects. In such circumstances, blueing effects, ultraviolet excess, circumstellar dust, gas shells, etc., may be present in and around the cluster members. It is therefore preferable to use the V band rather than the U and B bands, because in the optical region it is least affected by the spectral lines, etc., formed in such cases. Similarly, in the near-IR the J band is preferred because it minimizes contributions from the possible presence of circumstellar material, etc., around young stellar objects and also because this is the photometric band that best represents the emission from the stellar photosphere. We have therefore used $IE(V-J)$ in order to analyse the colour excess ratios. The colour excesses $IE(U-V)$, $IE(B-V)$, $IE(V-R)$, $IE(V-I)$, $IE(V-H)$ and $IE(V-K)$ are plotted against $IE(V-J)$ in Fig. 4, while $IE(V-L)$ versus $IE(V-J)$ and $IE(U-V)$ versus $IE(B-V)$ diagrams are shown in Fig. 5. The solid line represents the values of the ratios for the normal interstellar extinction law given by Mathis (1990). A few stars that deviate significantly from the solid line are marked.

An inspection of Figs 4 and 5 indicates the following.

(i) In the $IE(U-V)$, $IE(V-J)$ and the $IE(B-V)$, $IE(V-J)$ diagrams the number of stars below the solid line is

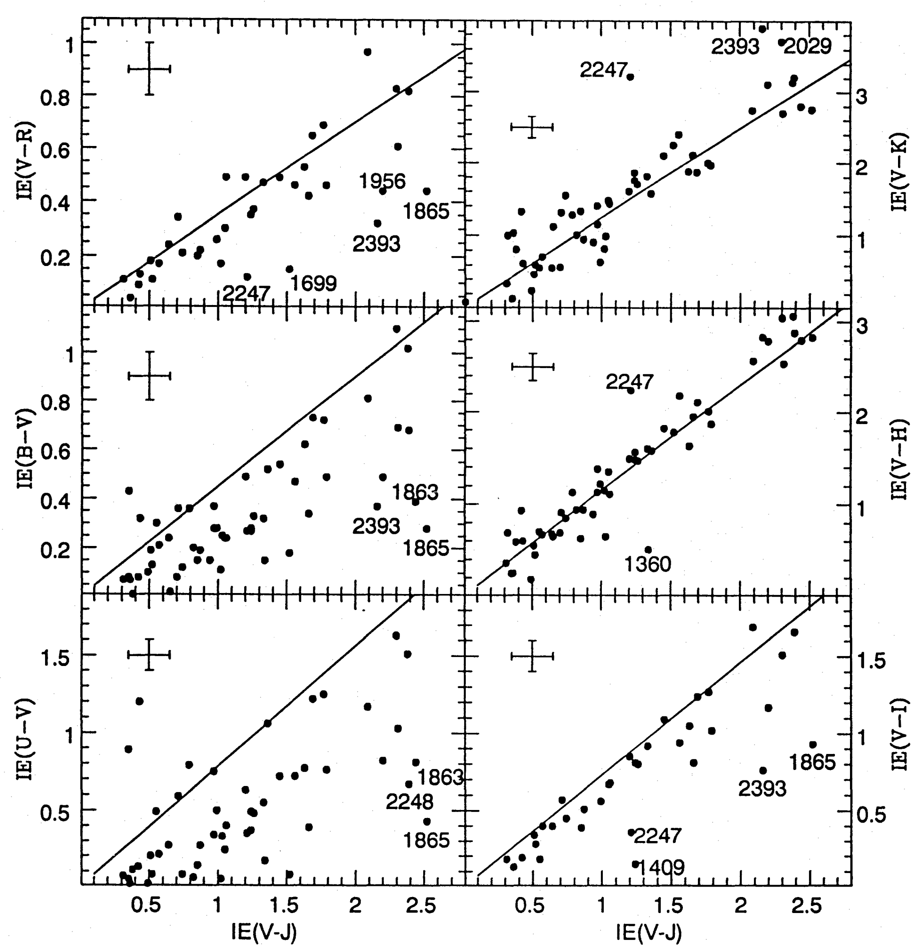

Figure 4. Plots of $IE(V-R)$, $IE(B-V)$, $IE(U-V)$, $IE(V-K)$, $IE(V-H)$ and $IE(V-I)$ against $IE(V-J)$. The solid lines show the reddening directions characteristic of a normal interstellar extinction law. Stars discussed in the text are marked. The lengths of the crosses represent the observational errors.

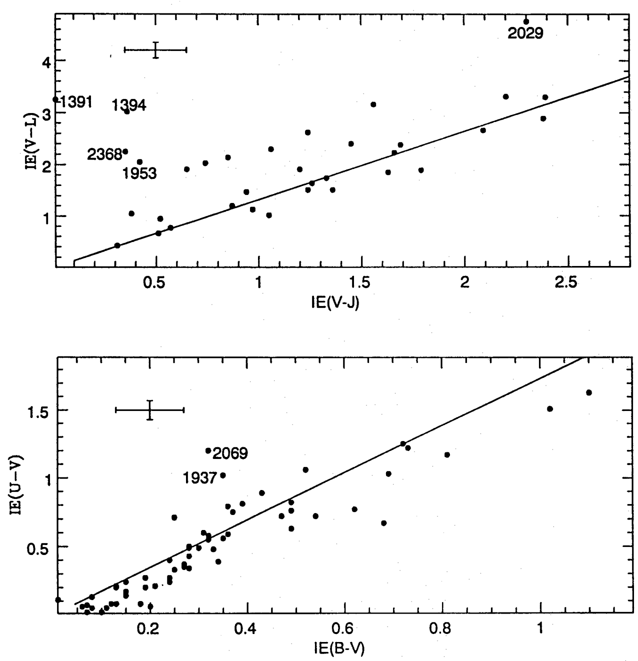

Figure 5. The $IE(V-L)$ versus $IE(V-J)$ and $IE(U-V)$ versus $IE(B-V)$ diagrams. Symbols are the same as in Fig. 4.

overwhelmingly large. This may imply that the majority of stars do not follow the normal interstellar extinction law. The plot of $IE(U-V)$ against $IE(B-V)$, however, indicates the contrary.

(ii) In the $IE(V-R)$, $IE(V-J)$ and $IE(V-I)$, $IE(V-J)$ diagrams, a good number of data points are located near but below the solid line, while they are evenly distributed with relatively small scatter around the solid line in the $IE(V-H)$, $IE(V-J)$ and $IE(V-K)$, $IE(V-J)$ diagrams. However, more points lie above the solid line in the $IE(V-L)$, $IE(V-J)$ diagram.

In order to quantify the above impressions, the following analyses have been carried out.

(1) The values of R and various colour excess ratios have been derived for each star individually. To avoid the determinations being dominated by observational errors, only stars with $IE(B-V) \geq 0.20$ mag have been considered. The $IE(V-J)$ values for such stars are listed in Table 3.

(2) Whittet & van Breda (1980) suggest that, in the absence of complete data at long wavelengths, the approximation $R = 1.1E(V-K)/E(B-V)$ generally used to deduce R is relatively insensitive to the reddening law adopted. We have therefore used this relation to evaluate R, which is listed in Table 3. The values of R have a wide range. Breger et al.

Table 3. $IE(V-J)$, R and colour excess ratios for the intracluster material. σ is the standard deviation in the mean value.

Star	IE(V-J) (mag)	R±σ	$\frac{IE(U-V)}{IE(B-V)} \pm \sigma$	$\frac{IE(U-V)}{IE(V-J)} \pm \sigma$	$\frac{IE(B-V)}{IE(V-J)} \pm \sigma$	$\frac{IE(V-R)}{IE(V-J)} \pm \sigma$	$\frac{IE(V-I)}{IE(V-J)} \pm \sigma$	$\frac{IE(V-H)}{IE(V-J)} \pm \sigma$	$\frac{IE(V-K)}{IE(V-J)} \pm \sigma$	$\frac{IE(V-L)}{IE(V-J)} \pm \sigma$
1044	0.51	2.72±1.33	1.05±0.53	0.39±0.18	0.37±0.18	0.35±0.17	0.67±0.24	1.08±0.43	0.92±0.40	1.29±0.48
1049	1.36	3.32±0.55	2.04±0.31	0.78±0.10	0.38±0.07	—	—	1.16±0.17	1.15±0.17	1.11±0.16
1212	1.69	2.82±0.35	1.67±0.19	0.72±0.08	0.43±0.06	0.38±0.05	0.73±0.08	1.25±0.14	1.11±0.13	1.41±0.15
1409	1.24	7.31±1.92	1.75±0.50	0.40±0.07	0.23±0.06	—	0.12±0.06	1.19±0.19	1.50±0.22	2.11±0.28
1469	0.79	3.91±0.89	2.19±0.47	1.00±0.21	0.46±0.12	—	—	1.43±0.33	1.62±0.36	—
1539	1.77	3.06±0.38	1.74±0.19	0.71±0.07	0.41±0.05	0.39±0.05	0.72±0.07	1.14±0.13	1.13±0.13	—
1623	1.56	5.62±0.91	1.53±0.27	0.46±0.06	0.30±0.05	0.29±0.05	0.60±0.07	1.40±0.17	1.54±0.18	2.03±0.22
1683	0.71	4.00±0.90	1.64±0.37	0.83±0.20	0.51±0.15	0.48±0.14	0.80±0.20	1.28±0.34	1.85±0.44	—
1712	1.20	3.59±0.61	1.29±0.23	0.53±0.09	0.41±0.08	0.41±0.08	0.71±0.11	1.24±0.20	1.33±0.21	1.59±0.23
1736	1.66	6.83±1.49	1.15±0.31	0.23±0.05	0.20±0.05	0.25±0.05	0.49±0.06	1.17±0.14	1.27±0.15	1.34±0.15
1772	1.33	6.22±1.46	1.72±0.43	0.41±0.07	0.24±0.06	0.35±0.07	0.69±0.09	1.20±0.18	1.36±0.19	1.31±0.19
1798	1.45	4.28±0.63	1.33±0.22	0.50±0.07	0.37±0.06	0.34±0.06	0.75±0.09	1.26±0.17	1.45±0.18	1.66±0.20
1799	2.38	3.39±0.28	1.48±0.12	0.63±0.05	0.43±0.04	—	—	1.29±0.10	1.32±0.10	1.21±0.10
1854	0.97	4.52±1.27	1.21±0.39	0.35±0.09	0.29±0.08	—	—	1.16±0.24	1.19±0.24	1.16±0.24
1863	2.44	7.90±1.48	2.08±0.41	0.33±0.04	0.16±0.03	—	—	1.15±0.09	1.15±0.09	—
1865	2.52	10.80±2.76	1.54±0.46	0.17±0.03	0.11±0.03	0.17±0.03	0.37±0.04	1.12±0.09	1.09±0.09	—
1885	1.05	6.74±2.08	1.00±0.41	0.23±0.07	0.23±0.07	0.29±0.08	0.64±0.11	1.29±0.23	1.40±0.25	0.97±0.20
1889	1.26	5.67±1.30	1.45±0.37	0.38±0.07	0.26±0.06	0.29±0.07	0.63±0.09	1.17±0.18	1.35±0.20	1.30±0.20
1891	1.24	7.13±1.95	1.37±0.44	0.30±0.07	0.22±0.06	0.28±0.07	0.65±0.10	1.26±0.19	1.41±0.21	1.22±0.19
1955	0.55	2.05±0.73	1.63±0.45	0.89±0.27	0.55±0.20	—	0.33±0.16	1.27±0.44	1.02±0.39	—
1956	2.20	6.98±1.05	1.67±0.28	0.37±0.04	0.22±0.04	0.20±0.03	0.53±0.05	1.27±0.11	1.41±0.12	1.50±0.12
1993	0.87	5.50±2.20	1.42±0.64	0.31±0.10	0.22±0.09	0.25±0.09	0.59±0.13	1.08±0.25	1.09±0.26	1.38±0.29
2029	2.30	3.71±0.28	1.48±0.11	0.71±0.06	0.48±0.04	0.36±0.04	0.66±0.05	1.32±0.11	1.61±0.12	2.07±0.15
2033	0.82	5.56±2.11	0.30±0.37	0.07±0.09	0.24±0.10	—	—	1.15±0.28	1.23±0.29	—
2069	0.43	2.13±0.70	3.75±0.85	2.79±0.99	0.74±0.31	0.30±0.19	—	1.40±0.60	1.44±0.61	—
2074	1.79	4.42±0.72	1.55±0.26	0.42±0.05	0.27±0.05	0.26±0.04	0.57±0.06	1.04±0.12	1.10±0.12	1.06±0.12
2100	0.97	4.16±0.90	2.03±0.43	0.77±0.14	0.38±0.09	—	—	1.42±0.27	1.44±0.27	—
2181	1.06	6.55±2.03	1.67±0.57	0.38±0.08	0.23±0.07	0.46±0.09	0.64±0.11	1.05±0.20	1.35±0.24	2.17±0.34
2244	0.99	2.51±0.86	1.79±0.51	0.51±0.10	0.28±0.08	0.26±0.08	0.57±0.11	1.23±0.24	0.65±0.18	—
2247	1.21	13.12±3.46	1.30±0.42	0.29±0.07	0.22±0.06	0.10±0.06	0.30±0.07	1.85±0.26	2.66±0.35	—
2248	2.39	5.19±0.59	0.99±0.14	0.28±0.03	0.28±0.03	0.34±0.04	0.69±0.05	1.21±0.10	1.34±0.11	1.38±0.11
2302	0.57	3.72±1.47	1.00±0.47	0.37±0.16	0.37±0.16	0.30±0.15	0.70±0.22	1.18±0.41	1.25±0.42	1.35±0.44
2317	1.03	4.36±1.39	1.32±0.46	0.32±0.08	0.24±0.08	—	—	0.63±0.17	0.96±0.20	—
2368	0.35	3.72±0.38	2.07±0.37	2.54±1.11	1.23±0.56	—	—	—	—	6.43±2.79
2393	2.16	11.56±2.23	—	—	0.17±0.03	0.15±0.03	0.35±0.04	1.31±0.11	1.80±0.14	2.87±0.21
2425	2.09	3.72±0.38	1.44±0.15	0.56±0.05	0.39±0.04	0.46±0.05	0.81±0.07	1.23±0.11	1.31±0.12	1.27±0.12
2476	2.31	4.30±0.50	1.49±0.18	0.45±0.04	0.30±0.04	0.26±0.03	—	1.10±0.10	1.17±0.10	—
2500	0.64	2.57±1.02	1.12±0.44	0.42±0.15	0.38±0.14	0.38±0.14	0.62±0.18	1.06±0.34	0.88±0.31	—
2519	1.63	3.34±0.46	1.24±0.18	0.47±0.06	0.38±0.06	0.33±0.05	0.64±0.07	1.00±0.13	1.15±0.14	1.13±0.14

Table 4. A comparison of the extinction law for the intracluster material with the normal interstellar extinction law given by van de Hulst (1949) curve No. 15 (see Johnson 1968) and by Cardelli et al. (1989).

Source	$\frac{E(U-V)}{E(V-J)}$	$\frac{E(B-V)}{E(V-J)}$	$\frac{E(V-R)}{E(V-J)}$	$\frac{E(V-I)}{E(V-J)}$	$\frac{E(V-H)}{E(V-J)}$	$\frac{E(V-K)}{E(V-J)}$	$\frac{E(V-L)}{E(V-J)}$
van de Hulst curve No. 15	0.75	0.43	0.35	0.70	1.13	1.21	1.27
Cardelli *et al.*	0.78	0.45	0.35	0.73	1.15	1.24	1.32
Group 1 stars	0.62±0.02	0.41±0.02	0.40±0.02	0.73±0.03	1.24±0.05	1.26±0.05	1.30±0.06
Group 2 stars	0.31±0.01	0.22±0.01	0.25±0.01	0.51±0.02	1.15±0.03	1.22±0.04	1.29±0.05
All stars	0.39±0.01	0.28±0.01	0.27±0.01	0.54±0.01	1.19±0.03	1.27±0.03	1.40±0.03

(1981) also derived values of R for 13 of our stars, with which our R values agree very well. For stars 1409, 1623, 1736, 1772, 1787, 1863, 1865, 1891, 1956, 2247, 2248 and 2393 the values of R are larger by more than 2σ than the normal value of 3.1. This is similar to the case of dense molecular clouds such as Ophiuchus or Taurus, where the values of R are in the range 4–6.

(3) The values of the colour excess ratios relative to $IE(V-J)$ as well as the value of the $IE(U-V)/IE(B-V)$ ratio, along with their σ, are listed in Table 3. For all stars, the value of the $IE(U-V)/IE(B-V)$ ratio generally agrees within 3σ with the value given for the normal interstellar extinction law. Based on the values of colour excess ratios, we can classify the stars into the following three groups. *Group 1:* stars 1044, 1049, 1212, 1469, 1539, 1683, 1712, 1798, 1799, 1955, 2069, 2100 and 2425 belong to this group, and the values of their colour excess ratios are in good agreement with the corresponding values for a normal interstellar extinction law at all wavelengths. *Group 2:* the values of the colour excess ratios for the stars in this group imply a normal interstellar extinction law at *JHKL* wavelengths, but an anomalous extinction law at *UBVRI* wavelengths in the sense that the values of the colour excess ratios are smaller than the corresponding normal values. Stars 1409, 1736, 1772, 1854, 1863, 1865, 1885, 1889, 1891, 1956, 1993, 2033, 2074, 2248, 2302, 2476, 2500 and 2519 belong to this group. *Group 3:* stars 1623, 2029, 2181, 2244, 2247, 2317, 2368 and 2393 are in this group. For these stars, the values of either optical or near-IR or both colour excess ratios are generally peculiar in the sense that known types of intracluster material cannot explain them. All these stars are either variable, or spectroscopic peculiar, or both. Most of them have Hα in emission. Flux deficiency or excess has also been seen in all of them (see Section 5). Since optical and near-IR observations were not simultaneous for the variable stars, it is possible that their *UBVRI* and *JHKLM* data were obtained at different brightness levels. This may be the cause of the observed peculiar colours and colour excess ratios in these stars. The weighted mean values of the colour excess ratios obtained for groups 1 and 2 and for all stars under discussion are listed in Table 4. For comparison, the colour excess ratios derived from curve 15 of van de Hulst (1949; see Johnson 1968) and those given by Cardelli et al. (1989) for the normal interstellar extinction law are also listed in the table. Of the three sets of mean values of the colour excess ratios, only the values for the group 1 stars are close to the corresponding normal values. This may imply the presence of anomalous intracluster extinction in the vicinity of many stars. The anomaly is due to the reduced extinction at U, B, R and I wavelengths and is similar to those observed by Smith (1987) and Tapia et al. (1988) in the direction of Carina nebula clusters and by Sagar & Qian (1990) in the regions around stars 72 and 143 in IC 1805.

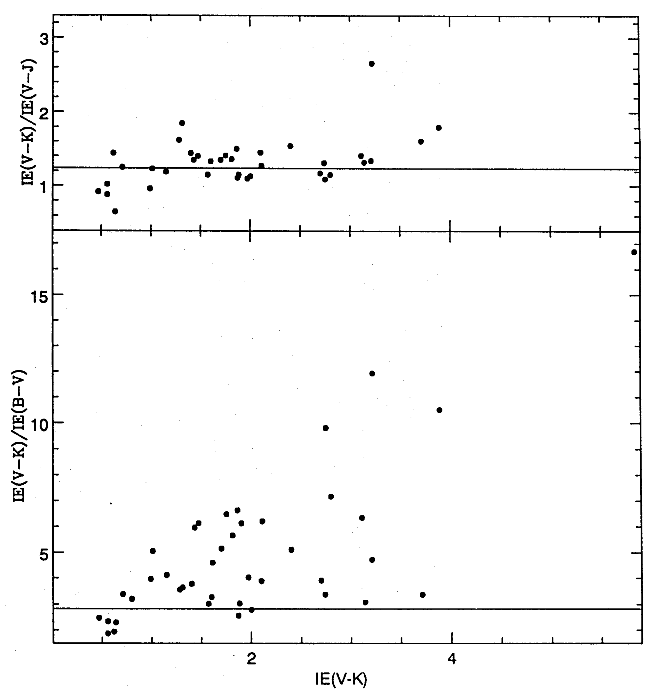

Figure 6. Plots of $IE(V-K)/IE(B-V)$ and $IE(V-K)/IE(V-J)$ against $IE(V-K)$. Values of the ratios for the normal interstellar extinction law are shown by horizontal lines.

(4) Following Tapia et al. (1988), the ratios $IE(V-K)/IE(B-V)$ and $IE(V-K)/IE(V-J)$ are plotted against $IE(V-K)$ in Fig. 6. The horizontal line in the diagram represents the value of the ratio for the normal interstellar extinction law given by Cardelli et al. (1989). In the case of an anomalous extinction law, the ratio $IE(V-K)/IE(B-V)$ varies significantly with the optical depth (Tapia et al. 1988), which is given by the value of $IE(V-K)$ here, while the value

of $IE(V-K)/IE(V-J)$ remains the same for all values of $IE(V-K)$. Least-squares linear fits to the data points yield

$$\frac{IE(V-K)}{IE(B-V)} = 1.93(\pm 0.30)\, IE(V-K) + 1.20(\pm 0.66), \qquad r = 0.72,$$

$$\frac{IE(V-K)}{IE(V-J)} = 0.17(\pm 0.05)\, IE(V-K) + 1.00 \pm (0.11), \qquad r = 0.47,$$

where r is the correlation coefficient of the linear fit. The values of both r and the slope indicate that only the ratio $IE(V-K)/IE(B-V)$ varies significantly with the value of $IE(V-K)$. This may therefore imply the presence of an anomalous intracluster extinction law.

5 NEAR-INFRARED FLUXES

It is well known that the presence of a circumstellar shell around young stars may be indicated by free–free excess radiation at wavelengths longward of about 1 μm. In order to quantify the presence of such radiation in the cluster members, the following simple analysis has been carried out.

The discussion in Section 4 indicates that both the interstellar extinction law in the direction of the cluster and the intracluster extinction law in the cluster are normal, in general, for wavelengths $\lambda \geq \lambda_I$, where $\lambda_I(\sim 0.9\ \mu m)$ is the effective wavelength of the I band. The combined extinction due to interstellar and intracluster material in the $(V-H)$, $(V-K)$, $(V-L)$ and $(V-M)$ colours is therefore derived individually for each star from the colour excesses $E(V-J)$, assuming the normal interstellar extinction law given by Cardelli et al. (1989). Based on the spectral classification of the cluster members, intrinsic colours are assigned using Koornneef's (1983) calibration. The differences between these and the corresponding observed intrinsic colours in $(V-H)$, $(V-K)$ and $(V-L)$ are plotted against $E(V-J)$ in Fig. 7, and indicate that:

(i) the scatter around the mean is independent of the amount of extinction indicated by the value of $E(V-J)$;

(ii) very few stars show an excess or a deficiency in the radiation at the H and K wavelengths, and

(iii) a significant number of stars have excess radiation at the L wavelength.

The major sources of error in the differences are (a) the observational uncertainties in the *JHKLM* magnitudes; (b) inaccuracies in the estimation of $E(V-J)$ and its ratios with $E(V-H)$, $E(V-K)$, $E(V-L)$ and $E(V-M)$; (c) uncertainty in the calibration of near-IR magnitudes, and (d) errors in the spectral and luminosity classifications. Consequently, the differences can be considered statistically significant only if their absolute values are larger than ~ 0.5 mag. Stars

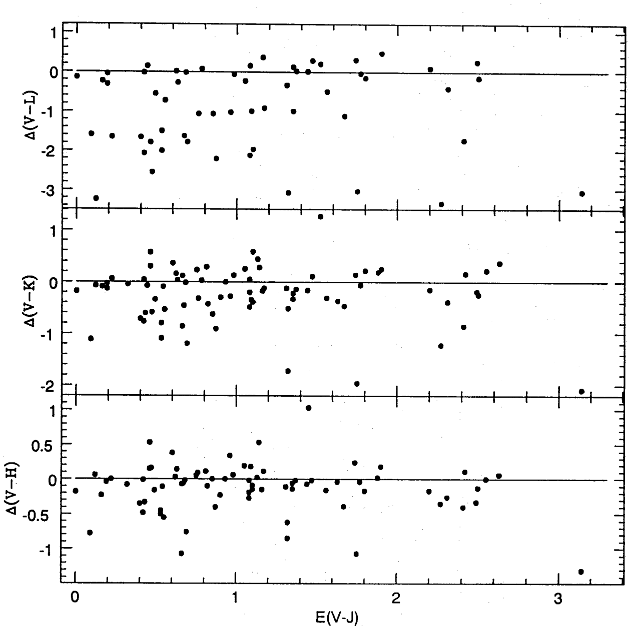

Figure 7. Plots of $\Delta(V-L)$, $\Delta(V-K)$ and $\Delta(V-H)$ against the colour excess $E(V-J)$. Horizontal lines denote zero-level differences.

Table 5. Near-infrared flux excess and deficiency. Δ is the spectral-type-calibrated colour minus the observed intrinsic colour, e.g. $\Delta(V-H)=(V-H)_{sp}-(V-H)_0$.

Star	E(V-J) (mag)	Δ(V-H) (mag)	Δ(V-K) (mag)	Δ(V-L) (mag)	Δ(V-M) (mag)
1044	0.62	0.03	0.16	0.01	-0.52
1076	0.09	-0.78	-1.11	-1.59	—
1270	0.49	-0.16	-0.34	-0.55	—
1360	1.45	1.03	—	—	—
1391	0.12	0.06	-0.07	-3.24	—
1394	0.47	0.16	-0.59	-2.55	—
1404	0.43	-0.33	-0.61	—	—
1409	1.35	-0.06	-0.33	-0.99	—
1606	0.85	0.00	-0.63	-1.06	-2.72
1623	1.67	-0.39	-0.47	-1.11	-1.60
1659	1.10	-0.15	-0.39	-1.97	—
1685	0.55	-0.55	-0.54	-0.72	—
1746	0.42	-0.48	-0.77	-2.07	—
1784	1.08	-0.19	-0.49	-2.12	—
1787	0.69	-0.76	-1.19	-1.78	—
1798	1.56	-0.16	-0.31	-0.49	—
1828	0.67	-0.06	-0.46	-1.63	—
1910	0.66	-1.07	-0.86	—	—
1937	3.14	-1.31	-2.09	-3.05	—
1953	0.53	-0.45	-0.80	-1.50	—
1956	2.31	-0.26	-0.39	-0.41	-1.00
2029	2.41	-0.40	-0.86	-1.73	-2.50
2032	1.32	-0.62	-0.52	—	—
2085	0.96	0.34	-0.28	-1.02	—
2086	0.40	-0.35	-0.72	-1.66	—
2181	1.17	0.11	-0.12	-0.91	—
2244	1.10	-0.09	0.58	—	—
2247	1.32	-0.85	-1.72	-3.07	-3.66
2312	1.09	0.18	-0.35	-0.99	—
2314	0.19	-0.04	-0.03	-0.05	-0.57
2317	1.14	0.53	0.28	—	—
2346	0.22	0.00	0.06	-1.65	—
2368	0.46	0.53	0.57	-1.79	—
2393	2.27	-0.35	-1.22	-3.34	—
2441	0.76	0.09	-0.32	-1.06	—
2473	0.53	-0.50	-1.09	-2.01	—
2479	1.75	-1.07	-1.96	-3.03	—
2510	0.87	-0.40	-0.91	-2.21	-3.50
2609	1.52	—	1.27	0.20	—

showing differences larger than this value in any of the passbands are listed in Table 5. All stars show excess radiation, which generally increases with wavelength from H to M, except stars 1360, 2244, 2317, 2368 and 2609, for which flux deficiency has been observed at either H or K or both wavelengths. Because of the flux excess or deficiency at H and/or K wavelengths for these stars, they occupy a peculiar (extreme right or left) position in the $(J-H)$ versus $(H-K)$ diagram (Fig. 2).

6 CONCLUSIONS

We have carried out *JHK* observations for 47 stars brighter than $V=14$ mag in the region of the Orion nebula cluster NGC 1976. Analysis of the present data in combination with near-IR and optical photometric and spectroscopic data yields the following main conclusions.

(1) The intracluster extinction law around many stars in the Orion nebula cluster is anomalous at U, B, R and I wavelengths and normal at wavelengths $\lambda > \lambda_I(\sim 0.9\ \mu m)$. The anomaly is such that it reduces extinction only in the U, B, R and I bandpasses, the values remaining normal for $IE(U-V)/IE(B-V)$ and near-IR colour excess ratios. This implies that in these regions the material responsible for extinction is less efficient at shorter wavelengths and that its grain size distribution is probably shifted by a small amount towards larger than normal sized particles. Breger et al. (1981) also arrived at the same conclusion independently using the relationship between the two grain-size indicators, the wavelength of maximum polarization (λ_{max}) and the ratio of total to selective absorption (R).

(2) Some stars show near-IR excess radiation, which generally increases with wavelength from H to M. This could be due to the presence of ~200-K heated dusty/gaseous regions around them (cf. Ney, Strecker & Gehrz 1973).

(3) Peculiar colours and colour excess ratios observed for some stars could be due to the presence of either variability or Hα emission, or both.

ACKNOWLEDGMENTS

We thank H. C. Bhatt and A. Subramaniam for critical reading of the manuscript. Useful comments given by the referee Dr M. Roth and the editor Dr P. M. Williams are gratefully acknowledged.

REFERENCES

Abt H. A., Wang R., Cardona O., 1991, ApJ, 367, 155
Breger M., 1976, ApJ, 204, 789
Breger M., Gehrz R. D., Hackwell J. A., 1981, ApJ, 248, 963
Brun A., 1935, Publ. Obs. Lyon, 1, No. 12
Cardelli J. A., Clayton G. C., Mathis J. S., 1989, ApJ, 345, 245
FitzGerald M. P., 1970, A&A, 4, 234
Gezari D. Y., Schmitz M., Mead J. M., 1987, in Catalog of infrared observations, 2nd edn, NASA Ref. Publ. No. 1196
Herbig G. H., Terndrup D. M., 1986, ApJ, 307, 609
Hu J. Y., 1986, in Sodakane K., Yamasaki A., eds, Proc. 2nd Japan–China workshop on stellar activities and observational techniques, Kyoto. University of Kyoto, Kyoto, p. 185
Johnson H. L., 1966, ARA&A, 4, 193
Johnson H. L., 1968, in Middlehurst B. M., Aller L. H., eds, Nebulae and Interstellar matter. Univ. Chicago Press, Chicago, Ch. 5
Jones B. F., Walker M. F., 1988, AJ, 95, 1755
Koornneef J., 1983, A&A, 128, 84
Lee T. A., 1968, ApJ, 152, 913
Levato H., Abt H. A., 1976, PASP, 88, 712
McNamara B. J., 1976, AJ, 81, 375
McNamara B. J., Huels S., 1983, A&AS, 54, 221
McNamara B. J., Hack W. J., Olson R. W., Mathieu R. D., 1989, AJ, 97, 1427
Mathis J. S., 1990, ARA&A, 28, 37
Mermilliod J.-C., 1992, Bull. Inf. CDS, 40, 115
Ney E. P., Strecker D. W., Gehrz R. D., 1973, ApJ, 180, 809
Panek R. J., 1983, ApJ, 270, 169
Parenago P. P., 1954, Trudy Sternberg Astron. Inst., Vol. 25
Penston M. V., 1973, ApJ, 183, 505
Roth M., 1988, MNRAS, 233, 773
Sagar R., 1987, MNRAS, 228, 483
Sagar R., Qian Z. Y., 1989, MNRAS, 240, 551
Sagar R., Qian Z. Y., 1990, ApJ, 353, 174
Schmidt-Kaler Th., 1982, in Schaifers K., Voigt M. M., eds, Landolt–Bornstein, Numerical data and functional relationships in science and technology, New Series, Group VI, Vol. 2(b). Springer-Verlag, Berlin, p. 14
Sharpless S., 1952, ApJ, 116, 251
Sharpless S., 1954, ApJ, 119, 200
Sharpless S., 1962, ApJ, 136, 767
Smith M. A., 1972, ApJ, 175, 765
Smith R. G., 1987, MNRAS, 227, 943
Tapia M., Roth M., Costero R., Navarro S., 1984, Rev. Mex. Astron. Astrofis., 9, 65
Tapia M., Roth M., Marraco H., Ruiz M. T., 1988, MNRAS, 232, 661
Tapia M., Costero R., Echevarria J., Roth M., 1991, MNRAS, 253, 649
Van Altena W. F., Lee J. T., Lee J. F., Lu P. K., Upgren A. R., 1988, AJ, 95, 1744
van de Hulst H. C., 1949, Rech. Astron. Obs. Utrecht, 11, Part 1, 1
Voshchinnikov N. V., Il'in V. B., 1987, SvA Lett, 13, 157
Walker M. F., 1969, ApJ, 155, 447
Walker M. F., 1983, ApJ, 271, 642
Warren W. H., Jr, Hesser J. E., 1977a, ApJS, 34, 115
Warren W. H., Jr, Hesser J. E., 1977b, ApJS, 34, 207
Whittet D. C. B., van Breda I. G., 1980, MNRAS, 192, 467